ACS Chemical Neuroscience

Research Article

pubs.acs.org/chemneuro

Binding Interactions of Dopamine and Apomorphine in D2High and D2Low States of Human Dopamine D2 Receptor Using Computational and Experimental Techniques

Serdar Durdagi,[*,†] Ramin Ekhteiari Salmas,[†,‡] Matthias Stein,[§] Mine Yurtsever,[‡] and Philip Seeman[*,∥]

[†]Department of Biophysics, School of Medicine, Bahcesehir University, 34349 Istanbul, Turkey

[‡]Department of Chemistry, Istanbul Technical University, 34469 Istanbul, Turkey

[§]Molecular Simulations and Design Group, Max-Planck Institute for Dynamics of Complex Technical Systems, Sandtorstrasse 1, 39106, Magdeburg, Germany

[∥]Departments of Pharmacology and Psychiatry, University of Toronto, 260 Heath Street West, Unit 605, M5P 3L6, Toronto, Ontario Canada

S *Supporting Information*

ABSTRACT: We have recently reported G-protein coupled receptor (GPCR) model structures for the active and inactive states of the human dopamine D2 receptor (D2R) using adrenergic crystal structures as templates. Since the therapeutic concentrations of dopamine agonists that suppress the release of prolactin are the same as those that act at the high-affinity state of the D2 receptor (D2High), D2High in the anterior pituitary gland is considered to be the functional state of the receptor. In addition, the therapeutic concentrations of anti-Parkinson drugs are also related to the dissociation constants in the D2High form of the receptor. The discrimination between the high- and low-affinity (D2Low) components of the D2R is not obvious and requires advanced computer-assisted structural biology investigations. Therefore, in this work, the derived D2High and D2Low receptor models (GPCR monomer and dimer three-dimensional structures) are used as drug-binding targets to investigate binding interactions of dopamine and apomorphine. The study reveals a match between the experimental dissociation constants of dopamine and apomorphine at their high- and low-affinity sites of the D2 receptor in monomer and dimer and their calculated dissociation constants. The allosteric receptor−receptor interaction for dopamine D2R dimer is associated with the accessibility of adjacent residues of transmembrane region 4. The measured negative cooperativity between agonist ligand at dopamine D2 receptor is also correctly predicted using the D2R homodimerization model.

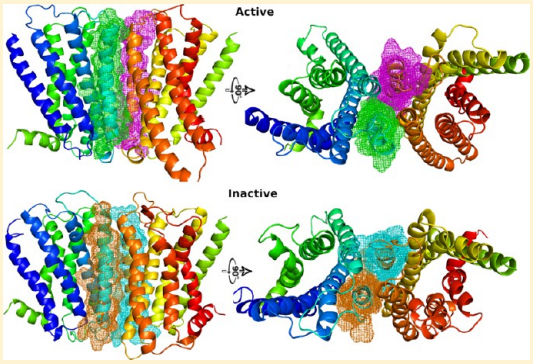

KEYWORDS: *Dopamine D2 receptor, protein engineering, molecular docking, D2High and D2Low states of dopamine, GPCR dimerization*

G-protein coupled receptors (GPCRs) represent the largest class of membrane proteins involved in signal transduction across biological membranes.[1] In parallel to the significant progress made in understanding the molecular mechanism, structure, and function of GPCRs, a growing number of discoveries have linked genetic mutations in these proteins with various diseases.[2] Because GPCR targets play fundamental roles in the regulation of membrane excitability, abnormalities in their structure disrupt the normal functioning of neurons, smooth muscle, and cardiac cells, leading to many genetic and acquired diseases such as neurodegenerative, cardiovascular, and renal diseases.[3] Therefore, finding therapeutic compounds that target GPCRs that are involved in such diseases is crucial. Dopamine receptors belong to the GPCR family, and they have a crucial role in cellular signaling in the human nervous system.[4,5] Dopamine receptors can exist in two forms, high affinity (D2High) or low affinity (D2Low), for dopamine.[4,5] Because the therapeutic concentrations of dopamine agonists that suppress the release of prolactin are the same as those that act at the high-affinity state of the D2 receptor (D2High), D2High in the anterior pituitary gland is considered to be the functional state of the receptor.[4,5] In addition, when considering anti-Parkinson drugs, it is known that the therapeutic concentrations of these drugs are related to the dissociation constants at the D2High form of the receptor.[6] One of the technical difficulties in measuring the affinities of dopamine agonists is that [^{3}H]spiperone has been used as a ligand for the D2 receptor.[7] This ligand, however, is very hydrophobic, highly soluble in membranes, and adheres tightly

Received: October 14, 2015
Accepted: December 8, 2015
Published: December 8, 2015

DOI: 10.1021/acschemneuro.5b00271
ACS Chem. Neurosci. 2016, 7, 185−195

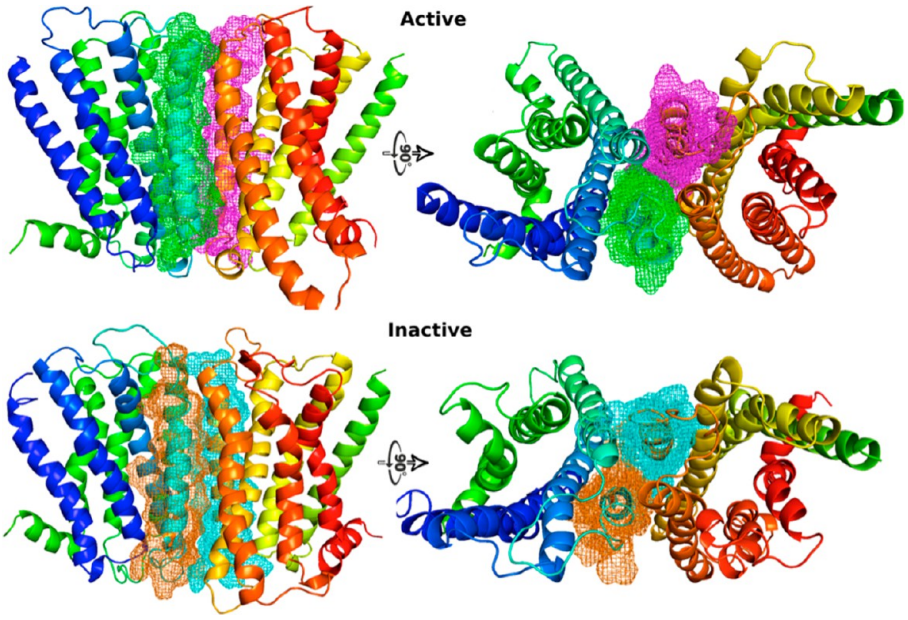

Figure 1. Active and inactive D2R models are constructed using experimental constraints and theoretical approaches. The receptor−receptor interactions for dopamine D2R are associated with the accessibility of adjacent residues of TM4, which are part of the homodimer interface. TM4 domains are highlighted via the electron density of their atoms.

to the D2 receptor, thereby yielding artifactually high dissociation constants (pM level), higher than those with the more water-soluble ligand [^{3}H]raclopride.[8] In fact, when competing various dopamine agonists against the [^{3}H]-spiperone ligand, the separation between the high- and low-affinity components is not always obvious and requires advanced computer-assisted drug binding studies.[9] It has been found, however, that the discrimination between the high- and low-affinity components for the D2 receptor (D2R) is much more reliable and clearly identifiable when using [^{3}H]-domperidone as a ligand for the D2 receptor.[10] The binding data of D2High and D2Low are similar when using [3H]raclopride and [3H]domperidone in the presence of a low concentration of sodium ions such as 10 mM NaCl. However, the presence of 120 mM NaCl reduces the number of D2High sites when using [3H]raclopride[11] but not when using [3H]domperidone.[12]

The objective of this study was to examine whether there was a match between the dissociation constants of dopamine and apomorphine drug molecules at their high- and low-affinity sites of the D2R, as determined from biological experiments, and their dissociation constants derived from the modeling data. Recent experimental evidence suggests that dimerization and oligomerization are important for the function of GPCRs.[13] In addition to the investigation of docking poses and interactions at the binding pockets of the D2R active and inactive monomers, the present work also includes protein engineering studies of D2R dimers and docking of dopamine and apomorphine to D2R dimers because such D2R dimers are known to be significantly elevated in the post-mortem human brain in schizophrenia.[14]

RESULTS AND DISCUSSION

Protein Engineering Studies of Active and Inactive D2R Models. 3D structures of the active and inactive states of monomer D2Rs were modeled using homology modeling approaches based on the full active and inactive X-ray structures of β2-adrenergic receptor. This receptor shares a reasonable amino acid sequence identity with unsolved D2R: 35% for the whole structure, 41% in the transmembrane (TM) regions, and 57% at the binding pocket of the protein. For individual conformers (active and inactive), 100 models were derived. Their backbone conformations were approximately the same with slight differences in side chain rotamers. Reasonable and proper models were selected by several validation tools (i.e., PROCHECK program[15] is used for Ramachandran's diagram,[16] steric hindrance, etc; in addition, docking simulations were used for reducing the number of models). In order to better understand the conformational deviations between derived active and inactive models, two conformers were superimposed. A distinct deviation to outward movement (around 13 Å) in the cytoplasmic half domain of TM6 was observed. In addition, the cytoplasmic sides of TM5 in the active and inactive states do not match well. This deviation and displacement in the cytoplasmic domains of TM5 and TM6 may be due to the coupling of G-protein to GPCR during the activation mechanism. In order to focus on the behavior of amino acid residues (backbone and side chains) that participate in the ligand binding pocket, the crucial amino acids involved in ligand−protein interactions (Asp114, Phe389, Phe390, Ser193, Ser194, Ser197, His393, Ile183, Trp386, Tyr408, and Tyr416) of active and inactive models were superimposed as shown in the Supporting Information (Figure S1). The results showed that in the case of Asp114 (TM3), which is the most important key amino acid in binding pocket, the backbone and side chain atoms have different orientations in both models. Together with Asp114, other residues, e.g., Ile183, Ser193, Ser194, and particularly Ser197, have been distinctively altered in all atoms.

Active and Inactive D2R Dimers. Following the investigation of drug−receptor binding of the active and inactive states of D2R monomers, receptor models of dimers of the active and inactive states of D2R were also constructed. This helped us to investigate and compare the obtained docking results using monomers and dimers with experimental

DOI: 10.1021/acschemneuro.5b00271
ACS Chem. Neurosci. 2016, 7, 185−195

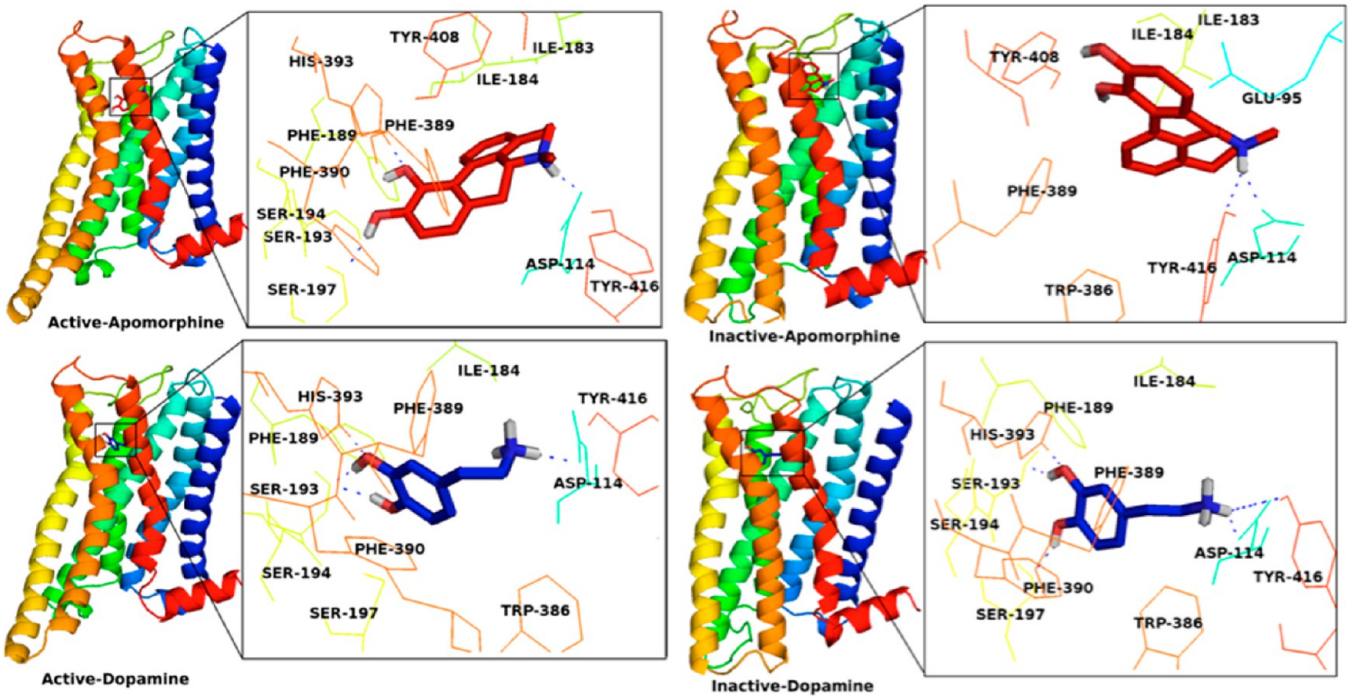

Figure 2. Top docking poses from induced fit docking (IFD) simulations of D2R monomers were selected for this profile. Each TM is highlighted by a different color (TM I–VIII). TM cavities of individual complexes are shown in greater detail, and their key amino acid residues involved in hydrogen-bonding interactions are represented by blue dashes.

Table 1. IFD Scores and K_i Values Determined for Dopamine and Apomorphine at the Binding Pockets of Active/Inactive Dopamine D2 Models[a]

	D2High (active state)			D2Low (inactive state)		
	IFD (kcal/mol)			IFD (kcal/mol)		
compound	monomer	dimer	K_i (nM)	monomer	dimer	K_i (nM)
dopamine	−10.63	−8.74	6.10	−8.83	−7.48	3650.00
apomorphine	−11.50	−9.09	1.80	−9.17	−8.51	98.00

[a]Both monomer and dimer conformers were implemented.

results.[13,17−20] As stated in the Methods section, Guo et al.[21] and Lee et al.[22] suggested a crucial role of TM4 in the dimerization of D2R. The dimer conformers in both the active and inactive forms (i.e., active−active and inactive−inactive) were initially assembled and then submitted to 10 ns atomistic MD simulations to relax the atomic interactions. Representative structures (i.e., the frame that has the lowest RMSD with the average structure) from the last 1 ns of the MD trajectory frames (see Figures 1 and 2) were selected for further docking simulations. The TM4 domains in dimeric D2R are highlighted via density maps of selected atoms (Figure 1). Inspecting the models of the both active and inactive dimer structures, we found that TM4 plays a pronounced role in the interaction and dimerization of monomeric D2R subunits. The main interactions established between each TM4 of both dimeric models were identified using a protein−protein interaction protocol. In the case of the active model, hydrogen bonds between the following amino acids from two TM4 sites are observed: Ser147−Arg145, Ala188−Asn175, Arg151−Asp131, Tyr146−Arg150, and Ile166−Tyr192 in distances of 2.6, 2.7, 2.7, 2.7, and 2.8 Å, respectively. In the inactive model, Asn186 residues of chains A and B at a distance of 2.6 Å established a hydrogen bond from their side chains.

Binding Affinity Prediction of Dopamine and Apomorphine into the Ligand Binding Pocket of Active and Inactive D2R Models. Dopamine and apomorphine compounds as D2R agonists were used to calculate their interaction energies at the binding pocket of both the active and inactive states of the D2R models. An induced fit docking (IFD protocol) was used to increase the reliability of finding binding poses. This protocol assists with increasing the flexibility of atoms of the models at the active site and thus accurately positions the ligand with a reasonable orientation. After the preparation of dopamine and apomorphine as explained in the Methods section, these compounds were docked individually into the binding pockets of active and inactive D2R models.

Dopamine-D2High Binding in Monomers and Dimers of D2R. The dopamine ligand was docked into the ligand binding pocket of D2High using IFD approaches. IFD derives several complexes with various docking scores and docking poses. The average of the estimated docking scores was calculated. Dopamine has −10.63 kcal/mol predicted interaction energy (IFD docking score) at the active state model for the monomer. (Table 1) The calculated dissociation constant (K_i) value using the Gibbs free energy equation at a temperature of 300 K is 17.68 nM. The experimental result was 6.10 nM. Binding interactions of dopamine at the target

DOI: 10.1021/acschemneuro.5b00271
ACS Chem. Neurosci. 2016, 7, 185−195

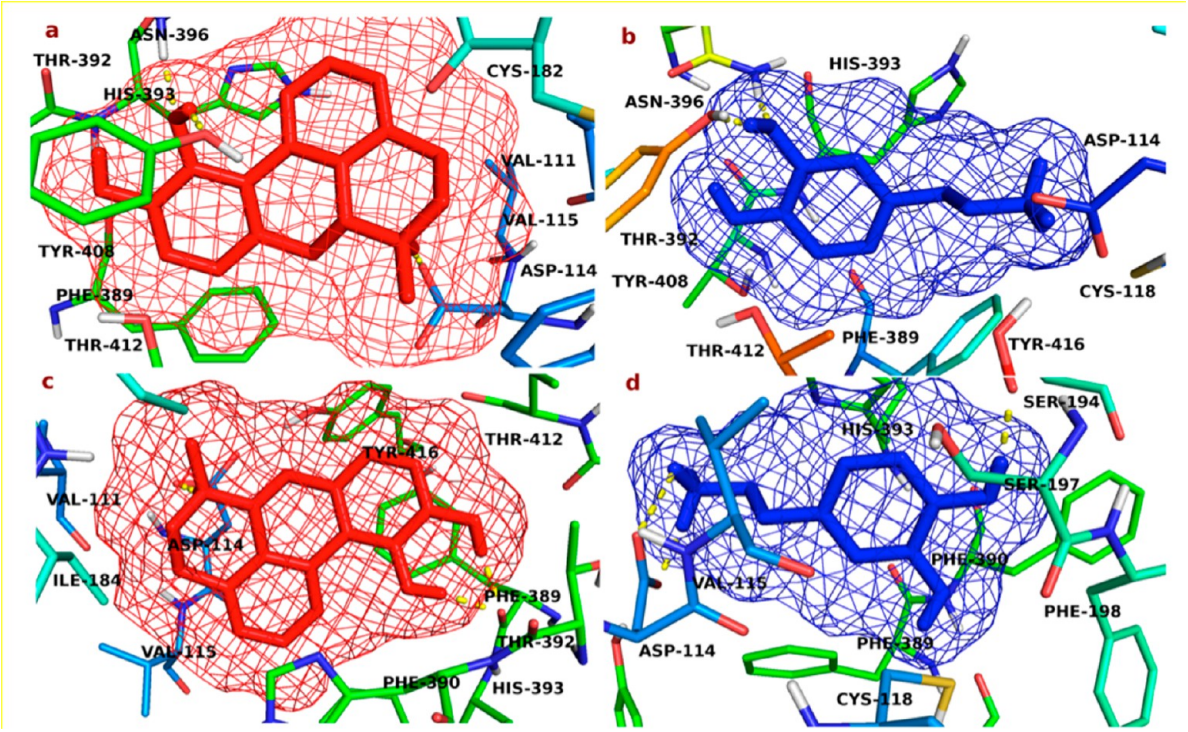

Figure 3. 3D docking poses of apomorphine and dopamine in the active site of active (a and b) and inactive (c and d) D2R dimers. Electron density of each ligand is illustrated via lines surrounding the atoms. The critical residues that make polar and nonpolar interactions with compounds are represented.

site are given in Figures 2 and 4. Dopamine forms strong hydrogen bonds with Asp114 (this bond is generally considered to be a salt bridge between a charged oxygen atom of Asp114 and protonated nitrogen atom of the ligand), Ser193, and His393. In addition to hydrogen-bonding interactions, His393 also establishes a $\pi-\pi$ stacking interaction with the aromatic ring of dopamine, as shown in Figure 4. IFD docking score of dopamine at the D2R dimer (active state form) was found to be −8.74 kcal/mol. (Table 1) The allosteric modulation (allosteric receptor−receptor interactions) for dopamine D2R is associated with the accessibility of adjacent residues of TM4, which are part of the homodimer interface. The negative cooperative interactions of the ligand at dopamine D2 receptors are consistent with the D2R homodimerization mode.[23] 3D and 2D ligand interaction diagrams are shown in Figures 3 and 4, respectively.

Apomorphine-D2High Binding in Monomers and Dimers of D2R. The binding affinity of apomorphine at the active site of the D2High model was calculated using the same protocol as that for dopamine, and the results are given in Table 1. This compound strongly binds to the D2R with a calculated interaction energy of −11.50 kcal/mol (the converted K_i value of predicted interaction energy was 4.10 nM). The experimental result of apomorphine at D2High was 1.80 nM. The top-docking pose of apomorphine at D2R (active state monomer model) is shown in Figure 3. As expected, Asp114 is establishing a strong hydrogen bond involved in the ligand−receptor interaction. Ser197 and His393 residues also participate in hydrogen bonding with dopamine. His393 formed a $\pi-\pi$ stacking interaction with the ligand (Figure 4). 2D ligand interaction diagrams also represent other hydrophobic interactions that play important roles in ligand binding. The IFD docking score of apomorphine at the active state of the D2R dimer was found to be −9.09 kcal/mol, which indicates tight binding, compared to the weak binder dopamine. However, apomorphine at the dimer has a lower docking score compared to its corresponding score at the monomer, as expected because of negative cooperativity (Table 1).

Dopamine-D2Low Binding in Monomers and Dimers of D2R. In addition to the active conformer, the inactive conformer was also tested to check the affinity of dopamine agonist at the active site of this model. Docking results show that dopamine exhibited the lowest (absolute) predicted interaction energy (−8.83 kcal/mol). The converted K_i value of the predicted interaction energy was 363.35 nM. The measured (experimental) K_i value of dopamine at D2Low was 3650.00 nM. 3D and 2D ligand interaction diagrams of dopamine at the binding cavity show that Asp114, Ser193, and Ser197 participate in forming hydrogen-bonding interactions with the ligand. His393 and Phe390 form $\pi-\pi$ stacking interactions with the aromatic ring of dopamine. The IFD docking score of dopamine at the D2R dimer (inactive state) was found to be −7.48 kcal/mol.

Apomorphine-D2Low Binding in Monomers and Dimers of D2R. The docking score of apomorphine at the inactive model of D2R was found to be −9.17 kcal/mol (converted predicted K_i and determined (experimental) values were 205.29 and 98.00 nM, respectively). Docking poses revealed that Asp114 and Ser409 establish hydrogen bonds with the protonated domain and charged oxygen atoms of apomorphine. This hydrogen bond alternates between Ser409 and Tyr408. The IFD docking score of apomorphine at the D2R dimer was found to be −8.51 kcal/mol.

In the current study, we tried to gain a better understanding of the binding interactions of dopamine and apomorphine at the D2High and D2Low states. Toward this end, a combined

DOI: 10.1021/acschemneuro.5b00271
ACS Chem. Neurosci. 2016, 7, 185−195

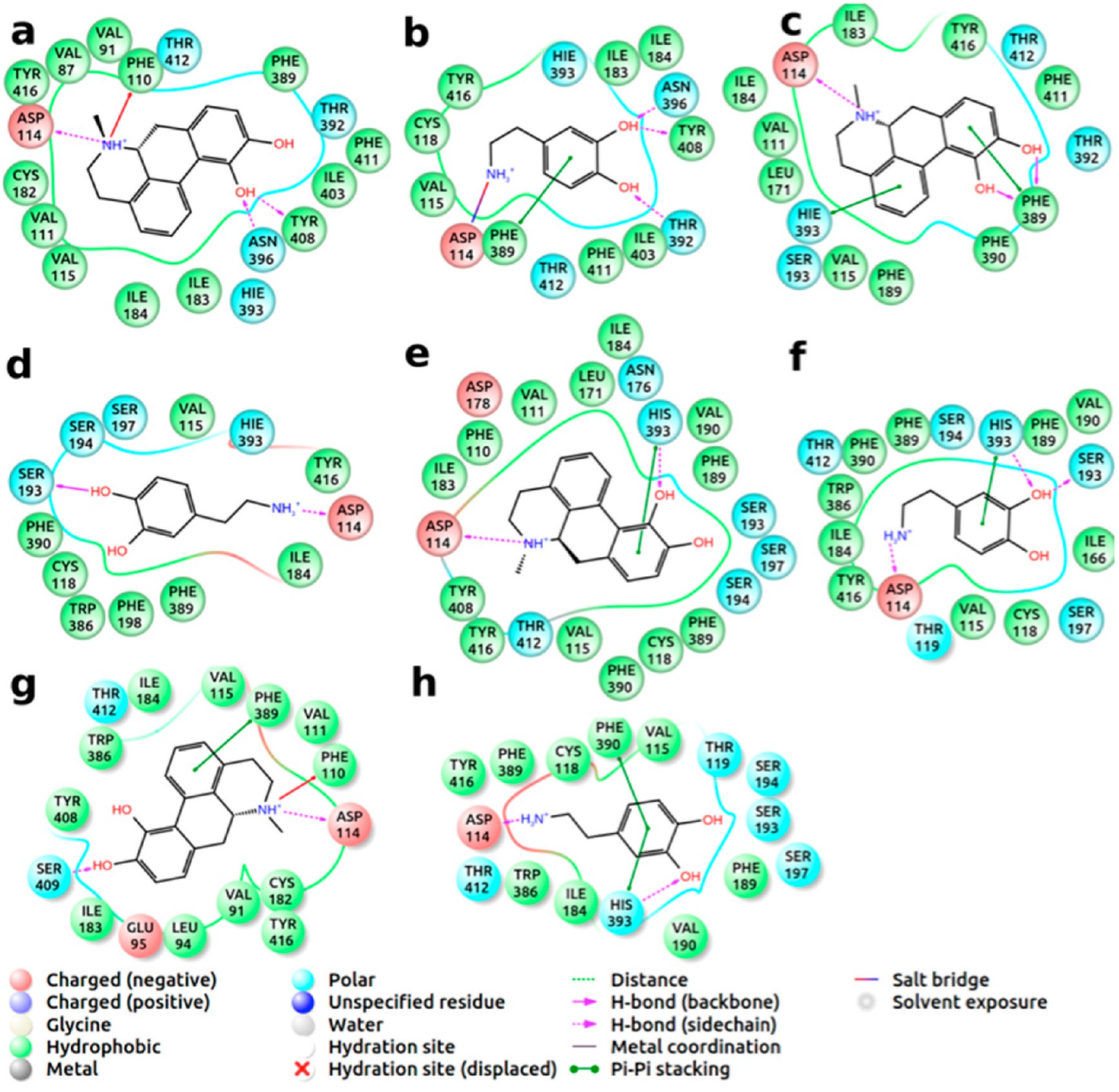

Figure 4. 2D ligand interaction diagrams for docking poses of apomorphine and dopamine in the active D2R dimer (a, b), inactive D2R dimer (c, d), active D2R monomer (e, f), and inactive D2R monomer (g, h) were diagrammed. Key amino acids within 4 Å of docked compounds and their binding interactions were identified.

experimental and theoretical study was performed. Experimental studies showed that dopamine inhibited the binding of [^{3}H]domperidone with dissociation constants of 6.1 ± 3.5 nM at D2High (or D2active) and 3650 ± 1600 nM at D2Low (or D2inactive). The dissociation constants of apomorphine were 1.8 ± 0.9 nM at D2High (or D2active) and 98 ± 40 nM at D2Low (or D2inactive) (Figure 5).

Our computational results are in good agreement with experimental results and reproduce the same trend in activity as that shown in Table 1. Figure 6 illustrates the superimposition of dopamine and apomorphine in the binding sites of the active and inactive models. The impact of conformational activity on the orientations and positions of docked compounds was studied. Dopamine in both the active and inactive monomeric models exhibits approximately the same conformational profile. However, in the case of apomorphine, a large difference was observed between the docked poses in the two states. Active and inactive dimeric D2Rs differently accommodated dopamine and apomorphine. Judging from the orientations of all docked compounds, we found that, in all cases, the protonated part of the molecule, which forms salt bridges with Asp114, shares approximately the same orientation (Figure 6).

Together with the Glide/IFD docking algorithm, we also used the flexible GOLD docking program. In order to obtain a reasonable statistical value from the docking scores, we used a very large sampling and derived 1000 docking poses for each compound. Figure 7 shows the docking scores (ChemScore) during the docking simulations. The average docking scores of

DOI: 10.1021/acschemneuro.5b00271
ACS Chem. Neurosci. 2016, 7, 185−195

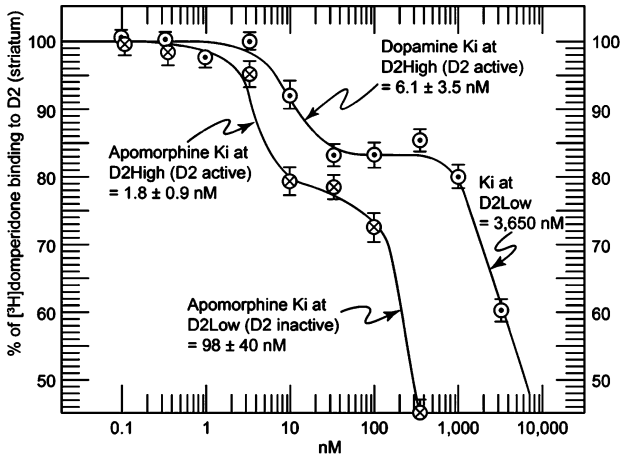

Figure 5. Competition of dopamine and apomorphine versus [^{3}H]domperidone at dopamine D2 receptors in homogenates of rat striata. There is a clear demarcation between competition at the high-affinity states of the receptors, at D2High (or D2active), and the low-affinity states of the receptors, at D2Low (or D2inactive). The average dissociation constants (K_i values; n = 5 independent experiments) were calculated by the Cheng–Prusoff equation from the concentrations that inhibited the high- and low-affinity components by 50%. Nonspecific binding defined by the presence of 10 μM S-sulpiride for D2. Data show competition between dopamine and apomorphine versus a final concentration of 2 nM [^{3}H]domperidone on dopamine D2 receptors in homogenates of rat striata. Data were averaged from four replicate experiments in our earlier study[6] and one additional replicate experiment that was subsequently done, for a total of five independent experiments in the current study.

dopamine at the active and inactive states for monomer D2R models were −17.32 and −17.40 kJ/mol, respectively. Corresponding values for apomorphine were −30.12 and −30.67 kJ/mol. The average docking scores of dopamine at the active and inactive states for dimer D2R models were −16.31 and −16.68 kJ/mol, respectively. Corresponding values for apomorphine were found to be −28.35 and −21.62 kJ/mol. The docking results showed that, compared to dopamine, apomorphine tightly binds to the D2R monomer target. However, both ligands have lower docking scores when they are targeted to dimers, as expected.

Per-residue Interaction Analysis. In order to clearly monitor the evolution of nonbonded interactions forming between compounds and active site residues of dimeric D2R throughout the MD simulations, atomistic interaction analysis was setup for each system. Hydrogen bond, hydrophobic, and ionic interactions as well as water bridges established in the ligand binding pocket were the main focus, and their occupancy interactions were calculated in each step of the simulation. The results are reported in stacked plots (Figure 8). As expected, Asp114 (a conserved amino acid; TM3) plays a significant role, forming hydrogen and ionic bonds with dopamine and apomorphine in both the active and inactive models. Figure 8a,b monitors the interactions occurring between dopamine and the protein in the inactive and active models. In both complexes, polar interactions are highly pronounced, and only Phe389 and Phe390 participate in hydrophobic connections. Figure 8c,d shows the interaction occupancies of apomorphine at the active and inactive D2R dimers, respectively. Val115 (TM3), Ile184 (ECL2), Phe389 (TM6), and Phe390 (TM6) contribute mainly to forming hydrophobic interactions with apomorphine in active D2R. Asp114, Ser193 (TM5), and Ser197 (TM5) are responsible for electrostatic interactions. Glu95 is the only amino acid from TM2 of the inactive dimeric model that forms an interaction with apomorphine.

CONCLUSIONS

In the current study, we measured the binding affinities of dopamine and apomorphine in the ligand binding pockets of active and inactive D2Rs with experimental and theoretical approaches. In addition, in the theoretical section we considered both the monomeric and dimeric forms of D2R in docking studies as well as MD simulations to examine the influence of dimerization on the active site. Our results are consistent with experimental observation that dimerization of D2R exhibits negative cooperativity on agonist ligand binding. In light of our theoretically and experimentally obtained results, dopamine and apomorphine exhibited higher absolute binding energies at D2High compared to those at D2Low. Dopamine

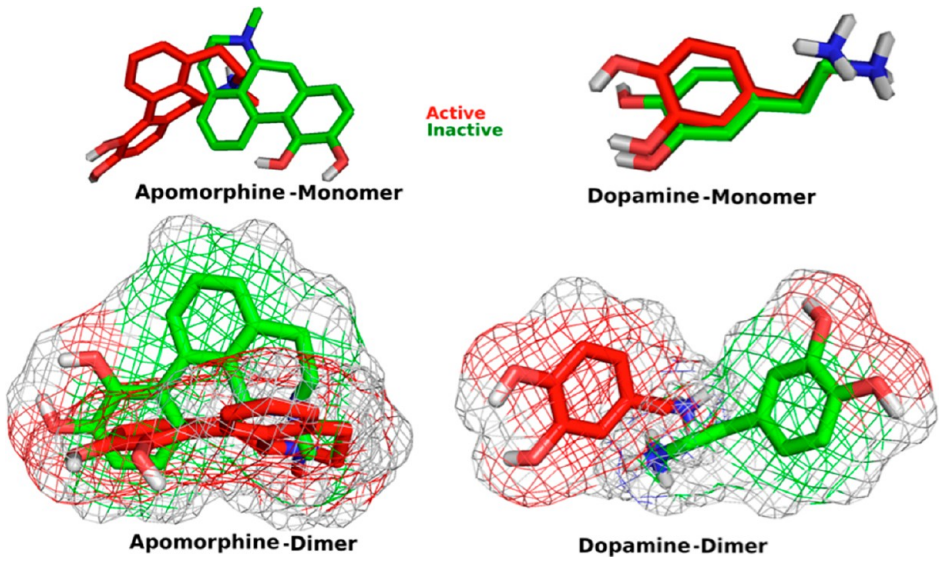

Figure 6. Superimposition of the top-docking poses of dopamine and apomorphine in active and inactive D2R monomer models.

DOI: 10.1021/acschemneuro.5b00271
ACS Chem. Neurosci. 2016, 7, 185–195

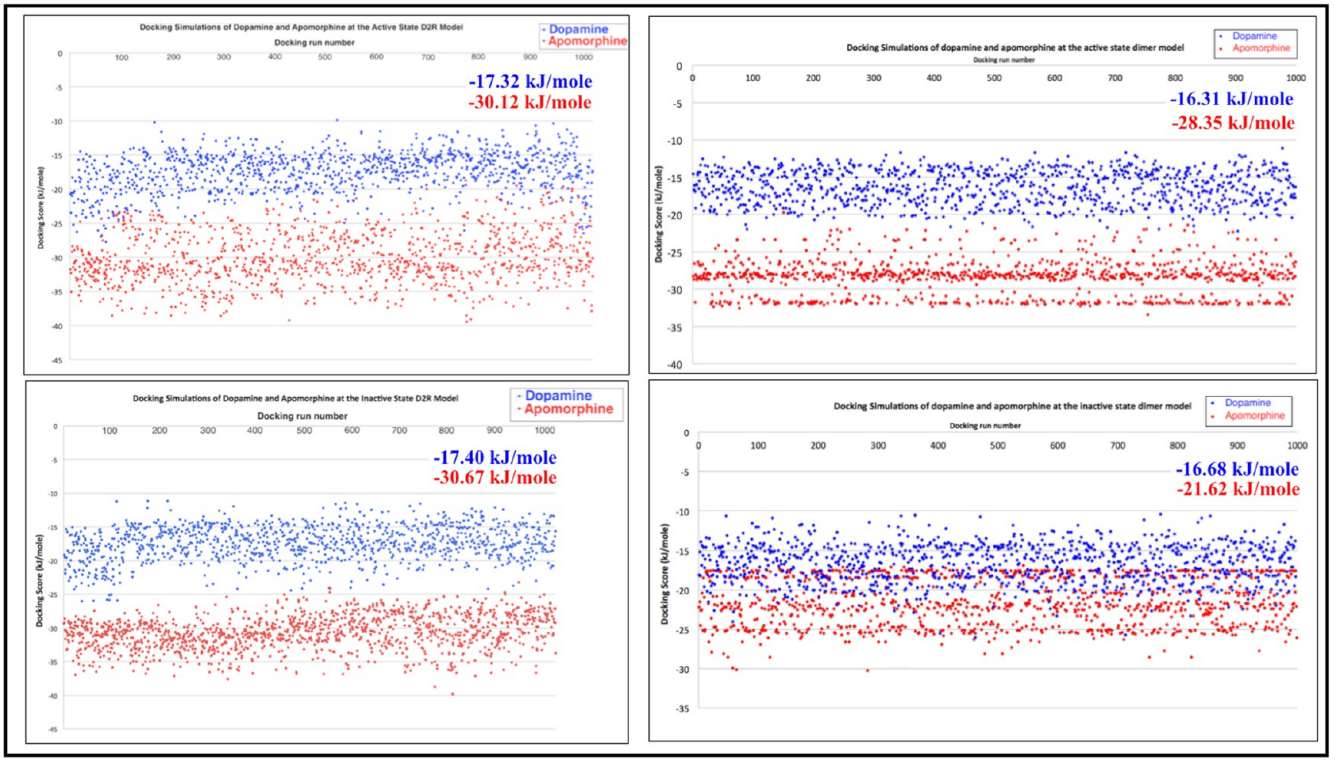

Figure 7. (left) Docking simulations of dopamine and apomorphine molecules at the active (top) and inactive states (bottom) for monomer D2R models. (right) Docking simulations of dopamine and apomorphine molecules at the active (top) and inactive states (bottom) for dimer D2R models. Each dot shows the binding score of a docking pose (in total, 1000 docking poses for each compound). Average docking scores of dopamine at the active and inactive states for monomer D2R models were found to be −17.32 and −17.40 kJ/mol, respectively. Corresponding values for apomorphine were found to be −30.12 and −30.67 kJ/mol. Average docking scores of dopamine at the active and inactive states for dimer D2R models were found to be −16.31 and −16.68 kJ/mol, respectively. Corresponding values for apomorphine were found to be −28.35 and −21.62 kJ/mol.

and apomorphine have higher binding affinities at the active states of D2R, which was verified by our models. In addition, it was correctly predicted by computational simulations that apomorphine binds more favorably, compared to dopamine, to both the D2High and D2Low conformers.

METHODS

Tissue Preparation. Rat striata were used from either carbon dioxide-euthanized Sprague−Dawley rats or from frozen rat brains (Pel-Freez Biologicals, Rogers, AR, USA). The brain (stored at −70 °C) was partly thawed, and the striatum was removed. The striata were homogenized in buffer (4 mg of frozen tissue per mL of buffer) using a Teflon-glass homogenizer (with the piston rotating at 500 rpm) and 10 up-and-down strokes of the glass container. The buffer contained 50 mM Tris-HC1 (pH 7.4 at 20 °C), 1 mM EDTA, 5 mM KCl, 1.5 mM $CaC1_2$, 4 mM $MgC1_2$, and 120 mM NaCl. The homogenate was not washed, centrifuged, or preincubated because previous work found that 30−50% of D2 receptors were lost by these procedures.[7]

Agonist/[^{3}H]Ligand Competition. The dopamine D2 receptors in the homogenized striata were measured with [^{3}H]domperidone (2 nM final concentration in the final incubation tube; prepared as [phenyl-^{3}H(N)]domperidone; 68 Ci/mmol; PerkinElmer Life Sciences Inc., Boston, MA).[7] Each incubation tube (12 × 75 mm, glass) received, in the following order, 0.5 mL of buffer (with or without a final concentration of 10 μM S-sulpiride to define nonspecific binding to the dopamine D2 receptors), 0.25 mL of [^{3}H]domperidone, and 0.25 mL of tissue homogenate. The tubes (total volume of 1 mL contents) were incubated for 2 h at room temperature (20 °C), after which the samples were filtered using a 12-well cell harvester (Titertek, Skatron, Lier, Norway) and buffer-presoaked glass fiber filter mats (Whatman GF/C). After filtering, the filter mat was rinsed with buffer for 15 s (7.5 mL buffer). The filters were pushed out and placed in scintillation minivials (7 mL, 16 × 54 mm; Valley Container Inc., Bridgeport, CT). The minivials received 4 mL each of scintillant (Research Products International Corp., Mount Prospect, IL) and were monitored 6 h later for tritium in a Beckman LS5000TA scintillation spectrometer at 55% efficiency. The specific binding of [^{3}H]domperidone was defined as total binding minus that in the presence of 10 μM S-sulpiride. The competition data were analyzed as previously described;[9,10] the program provided two statistical criteria to judge whether a two-site fit was better than a one-site fit or whether a three-site fit was better than a two-site fit.

Independently, the Cheng−Prusoff equation[24] was also used to derive the dissociation constants (K_i values) of the dopamine agonist from the concentration that inhibited 50% of the high-affinity component ($IC_{50\%}$) or 50% of the low-affinity component for [^{3}H]domperidone, as indicated in the results. The form of the Cheng−Prusoff equation used was $K_i = IC_{50}\%/(1 + C^*/K_d)$, where C^* is the final concentration of the radioligand and K_d is the dissociation constant of [^{3}H]domperidone (K_d = 0.43 nM), as determined directly by saturation binding (i.e., Scatchard plot) to the striatal homogenate.

Drugs. Apomorphine-*R*-(−)·HCl was generously provided by Merck Frosst Laboratories, Montreal (QC, Canada). Dopamine·HCl was purchased commercially.

Homology Modeling, Loop Modeling, and Protein Engineering Studies of D2R Monomers. 3D structures of D2R were modeled using active and inactive GPCR templates. Crystal structures of β2-adrenergic receptor in the full active (PDB ID: 3SN6[25]) and full inactive states (PDB ID: 3D4S[26]) were retrieved from Protein Data Bank. Water molecules and co-crystallized compounds were removed from the structures. Fusion fragments that are inserted in the third intracellular loop (ICL3) in both structures were excluded, and this domain was then modeled. Amino acid sequence information on D2R

DOI: 10.1021/acschemneuro.5b00271
ACS Chem. Neurosci. 2016, 7, 185−195

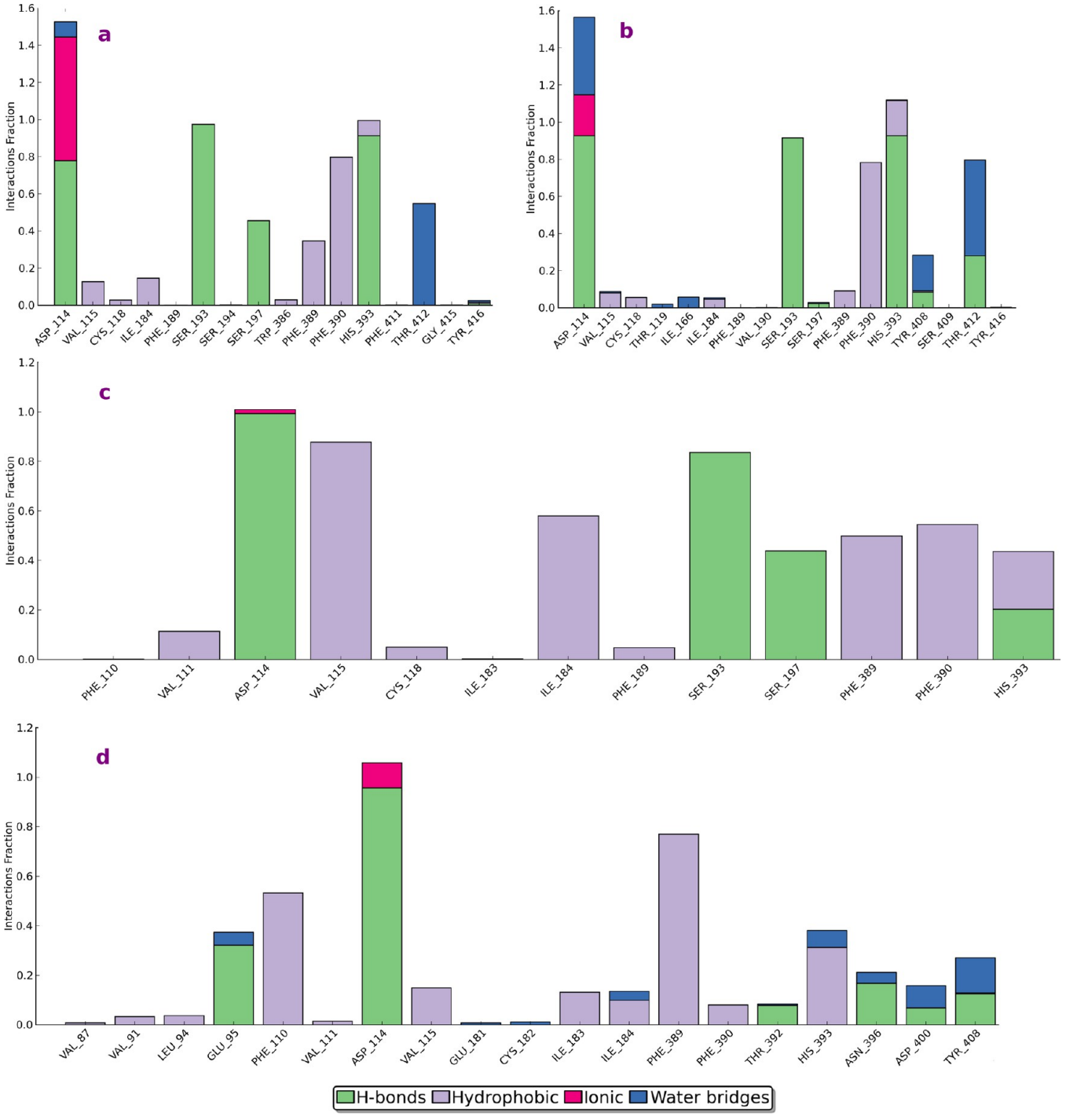

Figure 8. Per-residue interaction analysis of dopamine in the inactive and active dimeric D2R (a, b) and apomorphine at the active and inactive dimeric D2R (c, d). The fractions of the interactions that were hydrogen, hydrophobic, or ionic interactions or water bridges formed between ligands and critical amino acids at the binding pocket were calculated throughout the MD simulations.

in FASTA format was retrieved from the UniProtKB database[27] (code: P14416). Amino acid residues of ICL3 were excluded from sequence. Alignment between amino acids of the template (active and inactive states) and target were carried out using CLUSTALW. Details of the modeling and alignment process are described in our previous study.[28] The manually curated alignment was incorporated into MODELER 9.14.[29] ECL2 residues Asn186 and Ile184 in D2R were aligned with two residues (Thr195 and Phe193) from the templates, which point inward to the binding crevice. Then, extensive loop refinement modeling was carried out using ROSETTA loop modeling protocols.[30] A *de novo* fragment-based loop modeling tool was used to generate 20 000 conformers. The disulfide bridge between two cysteine residues in ECL2 (between Cys107 and Cys182) was constrained during the conformational search. Finally, hydrogen atoms were added to the homology models and a short energy minimization was carried out with the all-atom ROSETTA force field.[30] (Protonation states of amino acids were determined at physiological pH (pH 7.4) using PROPKA software.)[31] The top-100 models according to ROSETTA energy scores versus heavy atom RMSD values were selected. The top-10 lowest energy models are ranked on discrete optimized protein energy (DOPE) scores versus RMSD values, and the final models are selected based on available experimental results in the literature.

DOI: 10.1021/acschemneuro.5b00271
ACS Chem. Neurosci. 2016, 7, 185−195

Homology Modeling and Protein Engineering Studies of D2R Dimers. In order to investigate the influence of D2R dimerization on the ligand binding pocket, D2R dimers were atomistically modeled taking into account valuable information from experimental studies.[21−32] Guo et al.[21] and Lee et al.[22] investigated the homodimer interface in D2R over the entire length of the TM4 by site-directed cysteine mutants and suggested that TM4 plays a pivotal role in the dimerization of D2R. In addition, a theoretical model of rhodopsin (Rho) oligomer (PDB ID: 1N3M) was utilized in the construction of D2R dimers as a potential template.[32] The dimer conformers in both the active and inactive forms (i.e., active−active and inactive−inactive) were assembled. They were merged with a membrane bilayer, and then each of them was submitted to 10 ns atomistic MD simulations to relax the atomic interactions and remove steric clashes.

Molecular Dynamics (MD) Simulations. Both dimers (active−active and inactive−inactive conformations) were embedded into a 1-palmitoyl-2-oleoyl-*sn*-glycero-3-phosphocholine (POPC) membrane bilayer, and the dimer structures were placed in an orthorhombic box with layers of explicit TIP3P water molecules of 10 Å thickness.[33−38] The initial system of the inactive D2R dimer in complex with dopamine is shown in Figure 9. All MD simulations

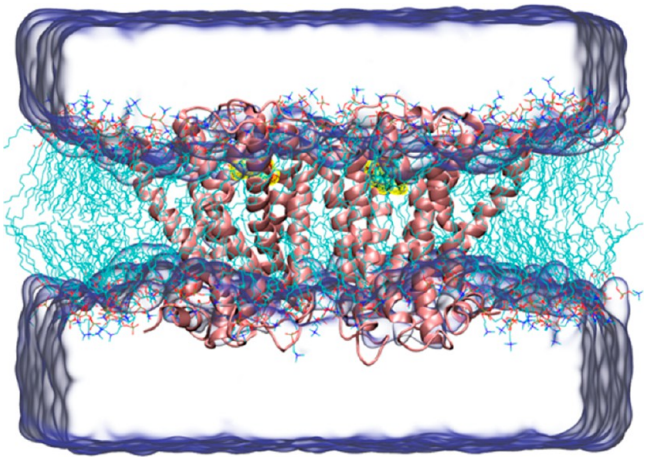

Figure 9. Inactive D2R dimer in complex with dopamine embedded into the membrane bilayer. Protein is shown by a cartoon model, and ligand and lipid molecules are shown in a CPK model. Water atoms are displayed in a quick surface model. VMD was used to generate the figure.

were carried out using the Desmond package.[39] The OPLS 2005 force field[40] was used to calculate the atomistic interactions. The particle-mesh Ewald method[41] was used to calculate the long-range electrostatic interactions. The short-range region for van der Waals interactions and short-range Coulombic interactions were defined by a cutoff radius of 9.0 Å. A Nosé−Hoover thermostat[42] and Martyna−Tobias−Klein method[43] were used to maintain the system at a temperature of 310 K and pressure of 1.01325 bar. A time step of 2.0 fs was used during the MD simulations. The systems were minimized for a maximum of 2000 iterations, and a convergence threshold of 1 kcal mol^{-1} $Å^{-1}$ was used. Both GPCR dimers were equilibrated using default algorithms of Desmond, which consist of several restrained simulations, to relax the system. Finally, four independent 10 ns atomistic MD simulations were setup as production runs.

Ligand Preparation. 3D structures of dopamine and apomorphine were constructed with the Macromodel module[44] of Maestro. Protonation states of each compound were assigned at physiological pH (pH 7.4) using the LigPrep module,[45] which it is implemented in Maestro.[46] In order to find the lowest and most populated conformational structure for each compound, the conformational search protocol of the MacroModel module[44] implemented in Maestro was employed.

Flexible Receptor Docking Protocol. Glide/IFD: The ligand binding pocket of the models (docking box) was identified by assignment of the critical amino acid residues (Asp114 (TM3), Trp386 (TM6), Phe390 (TM6), and Try416 (TM7)) from seven TM helical domains. In order to estimate the binding energy (i.e., docking score) of the compounds used in the active site of D2R, a flexible receptor docking simulation was used. For this, the IFD module[47] in Maestro was employed. The IFD protocol consists of three steps as follows: (i) flexible docking of the ligand into the active site using Glide/XP,[48] (ii) refining amino acid atoms within 4 Å of the ligand using Prime,[49] and (iii) redocking the ligand into the refined active site. Several docking poses were generated for individual ligands and sorted by their final docking scores and Prime energies. Target structures were superimposed in Figure 10.

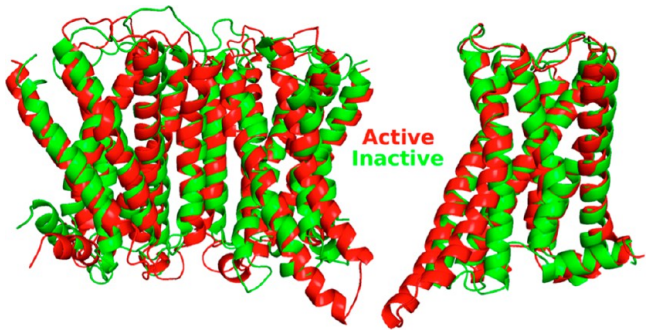

Figure 10. Superimposition of predicted active and inactive states of D2R dimer (left) and monomer (right). Active and inactive models are shown by red and green cartoons, respectively. Distinct deviation was observed at half of the cytoplasmic side of TM6. This domain in the active form moved outward from that in the inactive state in both the monomer and dimer conformers.

GOLD: The binding interactions were calculated using a genetic algorithm. In the genetic algorithm, the following steps are applied: (i) a population of potential binding poses at a defined binding pocket is set up at random; (ii) each member of the population is encoded as a "chromosome", which contains information about the mapping of protein−ligand interactions; (iii) each chromosome is assigned a fitness score based on its predicted binding affinity, and the chromosomes within the population are ranked according to fitness; and (iv) the population of chromosomes is iteratively optimized. In this work, the following genetic algorithm parameters were used (populations size, 1000; selection pressure,1.1; number of islands, 5; migrate, 10; mutate, 95; crossover, 95,; niche size, 2; and number of operations, 107 000). Default cutoff values of 2.5 Å (dH-X) for hydrogen bonds and 4.0 Å for van der Waals distance were employed. GoldScore fitness function and ChemScore[50] were used at the docking

$$\text{GoldScore fitness} = \text{Shb-ext} + \text{Svdw-ext} + \text{Shb-int+Svdw-int}$$

where Shb-ext is the protein−ligand hydrogen-bond score and Svdw-ext is the protein−ligand van der Waals score. Shb-int is the contribution to the fitness due to intramolecular hydrogen bonds in the ligand; Svdw-int is the contribution due to intramolecular strain in the ligand. On the other hand, the ChemScore function estimates the free energy of binding of the ligand to a protein

$$\Delta G_{\text{binding}} = \Delta G_0 + \Delta G_{\text{hbondShbond}} + \Delta G_{\text{metalSmetal}} + \Delta G_{\text{lipoSlipo}} + \Delta G_{\text{rotHrot}}$$

where Shbond, Smetal, and Slipo are scores for hydrogen-bonding, acceptor-metal, and lipophilic interactions, respectively. Hrot is a score representing the loss of conformational entropy of the ligand upon binding to the protein. The final ChemScore value is obtained by adding in a clash penalty and internal torsion terms, which militate against close contacts in docking and poor internal conformations. Covalent and constraint scores may also be included:

DOI: 10.1021/acschemneuro.5b00271
ACS Chem. Neurosci. 2016, 7, 185−195

$$\text{ChemScore} = \Delta G_{\text{binding}} + E_{\text{clash}} + E_{\text{int}}$$

In the GOLD docking algorithm,[51] one or more side chains of residues at the active site can be treated as flexible. Thus, 10 active site residues, Asp114, Cys118, Ser193, Ser194, Ser197, Phe198, His393, Tyr408, Thr412, and Tyr416, are treated as flexible. Each flexible side chain is allowed to undergo torsional rotations around one or more of its acyclic bonds during docking. Throughout the docking, the defined side chains are rotated in 10° increments and scanned over 360° with the aim of finding the optimized interactions between the docked ligand and receptor residue. In this way, the optimized side chain conformations of residues are determined.

■ ASSOCIATED CONTENT

Supporting Information

The Supporting Information is available free of charge on the ACS Publications website at DOI: 10.1021/acschemneuro.5b00271.

Superimposition of crucial amino acid residues at the binding pocket of active and inactive monomers (PDF)

■ AUTHOR INFORMATION

Corresponding Authors

*(S.D.) E-mail: serdar.durdagi@bahcesehir.edu.tr.

*(P.S.) E-mail: philip.seeman@utoronto.ca.

Author Contributions

S.D. and R.E.S. contributed equally to this work. S.D., M.Y., M.S., and P.S. participated in research design; S.D., R.E.S., and P.S. conducted experiments; all authors participated in data analysis and contributed to the writing of the manuscript.

Funding

This work was supported by the CIHR (Canadian Institutes of Health Research), Janet Marsh Frosst, David Medland, Pamela and Desmond O'Rorke in memory of John William Medland, and the estate of the late Dr. Karolina Jus. S.D. acknowledges support from Bilim Akademisi – The Science Academy, Turkey under the BAGEP program, and S.D. and M.Y. acknowledge TUBITAK ULAKBIM High Performance and Grid Computing Center (TR-Grid) as well as the National Center for High Performance Computing (Ulusal Yüksek Başarımlı Hesaplama Merkezi–UHeM) for support of computational sources. S.D. acknowledges CompecTA for their computational support and services. This work was financially supported by the Max Planck Society for the Advancement of Sciences and the 'Center for Dynamic Systems: Biosystems Engineering' by the state of Saxony-Anhalt.

Notes

The authors declare no competing financial interest.

■ ACKNOWLEDGMENTS

We thank Dr. H.-C. Guan for excellent technical assistance.

■ REFERENCES

(1) Audet, M., and Bouvier, M. (2012) Restructuring G-Protein-Coupled Receptor Activation. *Cell 151*, 14–23.

(2) Dror, R. O., Arlow, D. H., Maragakis, P., Mildorf, T. J., Pan, A. C., Xu, H., Borhani, D. W., and Shaw, D. E. (2011) Activation mechanism of the β2 -adrenergic receptor. *Proc. Natl. Acad. Sci. U. S. A. 108*, 18684–18689.

(3) Rosenbaum, D. M., Zhang, C., Lyons, J. a, Holl, R., Aragao, D., Arlow, D. H., Rasmussen, S. G. F., Choi, H.-J., Devree, B. T., Sunahara, R. K., Chae, P. S., Gellman, S. H., Dror, R. O., Shaw, D. E., Weis, W. I., Caffrey, M., Gmeiner, P., and Kobilka, B. K. (2011) Structure and function of an irreversible agonist-β(2) adrenoceptor complex. *Nature 469*, 236–240.

(4) McDonald, W. M., Sibley, D. R., Kilpatrick, B. F., and Caron, M. G. (1984) Dopaminergic inhibition of adenylate cyclase correlates with high affinity agonist binding to anterior pituitary D2 dopamine receptors. *Mol. Cell. Endocrinol. 36*, 201–9.

(5) George, S. R., Watanabe, M., Di Paolo, T., Falardeau, P., Labrie, F., and Seeman, P. (1985) The functional state of the dopamine receptor in the anterior pituitary is in the high affinity form. *Endocrinology 117*, 690–697.

(6) Seeman, P. (2007) Antiparkinson therapeutic potencies correlate with their affinities at dopamine D2High receptors. *Synapse 61*, 1013–1018.

(7) Seeman, P., Ulpian, C., Wreggett, K. a, and Wells, J. W. (1984) Dopamine receptor parameters detected by [3H]spiperone depend on tissue concentration: analysis and examples. *J. Neurochem. 43*, 221–35.

(8) Seeman, P., and Van Tol, H. H. (1995) Deriving the therapeutic concentrations for clozapine and haloperidol: the apparent dissociation constant of a neuroleptic at the dopamine D2 or D4 receptor varies with the affinity of the competing radioligand. *Eur. J. Pharmacol., Mol. Pharmacol. Sect. 291*, 59–66.

(9) Seeman, P., Watanabe, M., Grigoriadis, D., Tedesco, J. L., George, S. R., Svensson, U., Nilsson, J. L. G., and Neumeyer, J. L. (1985) Dopamine D2 receptor binding sites for agonists. A tetrahedral model. *Mol. Pharmacol. 28*, 391–399.

(10) Seeman, P., Tallerico, T., and Ko, F. (2003) Dopamine displaces [3H]domperidone from high-affinity sites of the dopamine D2 receptor, but not [3H]raclopride or [3H]spiperone in isotonic medium: Implications for human positron emission tomography. *Synapse 49*, 209–15.

(11) Seeman, P., Weinshenker, D., Quirion, R., Srivastava, L. K., Bhardwaj, S. K., Grandy, D. K., Premont, R. T., Sotnikova, T. D., Boksa, P., El-Ghundi, M., O'Dowd, B. F., George, S. R., Perreault, M. L., Männistö, P. T., Robinson, S., Palmiter, R. D., and Tallerico, T. (2005) Dopamine supersensitivity correlates with D2High states, implying many paths to psychosis. *Proc. Natl. Acad. Sci. U. S. A. 102*, 3513–3518.

(12) Seeman, P., Schwarz, J., Chen, J. F., Szechtman, H., Perreault, M., McKnight, G. S., Roder, J. C., Quirion, R., Boksa, P., Srivastava, L. K., Yanai, K., Weinshenker, D., and Sumiyoshi, T. (2006) Psychosis pathways converge via D2High dopamine receptors. *Synapse 60*, 319–46.

(13) Han, Y., Moreira, I. S., Urizar, E., Weinstein, H., and Javitch, J. a. (2009) Allosteric communication between protomers of dopamine class A GPCR dimers modulates activation. *Nat. Chem. Biol. 5*, 688–695.

(14) Wang, M., Pei, L., Fletcher, P. J., Kapur, S., Seeman, P., and Liu, F. (2010) Schizophrenia, amphetamine-induced sensitized state and acute amphetamine exposure all show a common alteration: increased dopamine D2 receptor dimerization. *Mol. Brain 3*, 25.

(15) Laskowski, R. a., MacArthur, M. W., Moss, D. S., and Thornton, J. M. (1993) PROCHECK: a program to check the stereochemical quality of protein structures. *J. Appl. Crystallogr. 26*, 283–291.

(16) Gopalakrishnan, K., Sowmiya, G., Sheik, S. S., and Sekar, K. (2007) Ramachandran plot on the web (2.0). *Protein Pept. Lett. 14*, 669–671.

(17) Roberts, D. J., and Strange, P. G. (2005) Mechanisms of inverse agonist action at D2 dopamine receptors. *Br. J. Pharmacol. 145*, 34–42.

(18) Guo, W., Shi, L., and Javitch, J. a. (2003) The fourth transmembrane segment forms the interface of the dopamine D2 receptor homodimer. *J. Biol. Chem. 278*, 4385–8.

(19) Castro, S. W., and Strange, P. G. (1993) Differences in the Ligand Binding Properties of the Short and Long Versions of the D2 Dopamine Receptor. *J. Neurochem. 60*, 372–375.

(20) Fotiadis, D., Liang, Y., Filipek, S., Saperstein, D. a, Engel, A., and Palczewski, K. (2003) Atomic-force microscopy: Rhodopsin dimers in native disc membranes. *Nature 421*, 127–128.

(21) Guo, W., Shi, L., Filizola, M., Weinstein, H., and Javitch, J. A. (2005) Crosstalk in G protein-coupled receptors: changes at the

DOI: 10.1021/acschemneuro.5b00271
ACS Chem. Neurosci. 2016, 7, 185–195

transmembrane homodimer interface determine activation. *Proc. Natl. Acad. Sci. U. S. A. 102*, 17495−17500.
(22) Lee, S. P., O'Dowd, B. F., Rajaram, R. D., Nguyen, T., and George, S. R. (2003) D2 dopamine receptor homodimerization is mediated by multiple sites of interaction, including an intermolecular interaction involving transmembrane domain 4. *Biochemistry 42*, 11023−11031.
(23) Armstrong, D., and Strange, P. G. (2001) Dopamine D2 receptor dimer formation: evidence from ligand binding. *J. Biol. Chem. 276*, 22621−22629.
(24) Cheng, Y., and Prusoff, W. H. (1973) Relationship between the inhibition constant (K1) and the concentration of inhibitor which causes 50% inhibition (I50) of an enzymatic reaction. *Biochem. Pharmacol. 22*, 3099−3108.
(25) Rasmussen, S. G. F., DeVree, B. T., Zou, Y., Kruse, A. C., Chung, K. Y., Kobilka, T. S., Thian, F. S., Chae, P. S., Pardon, E., Calinski, D., Mathiesen, J. M., Shah, S. T. a, Lyons, J. a, Caffrey, M., Gellman, S. H., Steyaert, J., Skiniotis, G., Weis, W. I., Sunahara, R. K., and Kobilka, B. K. (2011) Crystal structure of the β2 adrenergic receptor-Gs protein complex. *Nature 477*, 549−55.
(26) Hanson, M. A., Cherezov, V., Griffith, M. T., Roth, C. B., Jaakola, V.-P., Chien, E. Y. T., Velasquez, J., Kuhn, P., and Stevens, R. C. (2008) A specific cholesterol binding site is established by the 2.8 A structure of the human beta2-adrenergic receptor. *Structure 16*, 897−905.
(27) Boutet, E., Lieberherr, D., Tognolli, M., Schneider, M., and Bairoch, A. (2007) UniProtKB/Swiss-Prot. *Methods Mol. Biol. 406*, 89−112.
(28) Salmas, R. E., Yurtsever, M., Stein, M., and Durdagi, S. (2015) Modeling and protein engineering studies of active and inactive states of human dopamine D2 receptor (D2R) and investigation of drug/receptor interactions. *Mol. Diversity 19*, 321−32.
(29) Eswar, N., Webb, B., Marti-Renom, M. a, Madhusudhan, M. S., Eramian, D., Shen, M.-Y., Pieper, U., and Sali, A. (2007) Comparative protein structure modeling using MODELLER. *Curr. Protoc. Protein Sci.*, DOI: 10.1002/0471140864.ps0209s50.
(30) Das, R., and Baker, D. (2008) Macromolecular modeling with rosetta. *Annu. Rev. Biochem. 77*, 363−382.
(31) Bas, D. C., Rogers, D. M., and Jensen, J. H. (2008) Very fast prediction and rationalization of pKa values for protein-ligand complexes. *Proteins: Struct., Funct., Genet. 73*, 765−783.
(32) Fotiadis, D., Jastrzebska, B., Philippsen, A., Müller, D. J., Palczewski, K., and Engel, A. (2006) Structure of the rhodopsin dimer: a working model for G-protein-coupled receptors. *Curr. Opin. Struct. Biol. 16*, 252−9.
(33) Salmas, R. E., Yurtsever, M., and Durdagi, S. (2015) Investigation of Inhibition Mechanism of Chemokine Receptor CCR5 by Micro-second Molecular Dynamics Simulations. *Sci. Rep. 5*, 13180.
(34) Leonis, G., Avramopoulos, A., Salmas, R. E., Durdagi, S., Yurtsever, M., and Papadopoulos, M. G. (2014) Elucidation of conformational states, dynamics, and mechanism of binding in human κ-opioid receptor complexes. *J. Chem. Inf. Model. 54*, 2294−308.
(35) Durdagi, S., Papadopoulos, M. G., Zoumpoulakis, P. G., Koukoulitsa, C., and Mavromoustakos, T. (2010) A computational study on cannabinoid receptors and potent bioactive cannabinoid ligands: Homology modeling, docking, de novo drug design and molecular dynamics analysis. *Mol. Diversity 14*, 257−276.
(36) Potamitis, C., Zervou, M., Katsiaras, V., Zoumpoulakis, P., Durdagi, S., Papadopoulos, M. G., Hayes, J. M., Grdadolnik, S. G., Kyrikou, I., Argyropoulos, D., Vatougia, G., and Mavromoustakos, T. (2009) Antihypertensive drug valsartan in solution and at the AT1 receptor: conformational analysis, dynamic NMR spectroscopy, in silico docking, and molecular dynamics simulations. *J. Chem. Inf. Model. 49*, 726−39.
(37) Durdagi, S., Kapou, A., Kourouli, T., Andreou, T., Nikas, S. P., Nahmias, V. R., Papahatjis, D. P., Papadopoulos, M. G., and Mavromoustakos, T. (2007) The application of 3D-QSAR studies for novel cannabinoid ligands substituted at the C1′ position of the alkyl side chain on the structural requirements for binding to cannabinoid receptors CB1 and CB2. *J. Med. Chem. 50*, 2875−85.
(38) Agelis, G., Resvani, A., Durdagi, S., Spyridaki, K., Tůmová, T., Slaninová, J., Giannopoulos, P., Vlahakos, D., Liapakis, G., Mavromoustakos, T., and Matsoukas, J. (2012) The discovery of new potent non-peptide Angiotensin II AT1 receptor blockers: a concise synthesis, molecular docking studies and biological evaluation of N-substituted 5-butylimidazole derivatives. *Eur. J. Med. Chem. 55*, 358−74.
(39) (2009) *Desmond Molecular Dynamics System*, version 2.2, D.E. Shaw Research, New York.
(40) Siu, S. W. I., Pluhackova, K., and Böckmann, R. a. (2012) Optimization of the OPLS-AA force field for long hydrocarbons. *J. Chem. Theory Comput. 8*, 1459−1470.
(41) Essmann, U., Perera, L., Berkowitz, M. L., Darden, T., Lee, H., and Pedersen, L. G. (1995) A smooth particle mesh Ewald method. *J. Chem. Phys. 103*, 8577−8593.
(42) Hoover, W. G. (1985) Canonical dynamics: Equilibrium phase-space distributions. *Phys. Rev. A: At., Mol., Opt. Phys. 31*, 1695−1697.
(43) Martyna, G. J., Tobias, D. J., and Klein, M. L. (1994) Constant pressure molecular dynamics algorithms. *J. Chem. Phys. 101*, 4177.
(44) (2014) *MacroModel*, version 10.6, Schrödinger, LLC, New York.
(45) (2014) *LigPrep*, version 3.2, Schrödinger, LLC, New York.
(46) (2014) *Maestro*, version 10.0, Schrödinger, LLC, New York.
(47) Farid, R., Day, T., Friesner, R. A., and Pearlstein, R. A. (2006) New insights about HERG blockade obtained from protein modeling, potential energy mapping, and docking studies. *Bioorg. Med. Chem. 14*, 3160−3173.
(48) Friesner, R. a., Murphy, R. B., Repasky, M. P., Frye, L. L., Greenwood, J. R., Halgren, T. a., Sanschagrin, P. C., and Mainz, D. T. (2006) Extra precision glide: Docking and scoring incorporating a model of hydrophobic enclosure for protein-ligand complexes. *J. Med. Chem. 49*, 6177−6196.
(49) Jacobson, M. P., Pincus, D. L., Rapp, C. S., Day, T. J. F., Honig, B., Shaw, D. E., and Friesner, R. a. (2004) A Hierarchical Approach to All-Atom Protein Loop Prediction. *Proteins: Struct., Funct., Genet. 55*, 351−367.
(50) Annamala, M. K., Inampudi, K. K., and Guruprasad, L. (2007) Docking of phosphonate and trehalose analog inhibitors into M. tuberculosis mycolyltransferase Ag85C: Comparison of the two scoring fitness functions GoldScore and ChemScore, in the GOLD software. *Bioinformation 1*, 339−50.
(51) Verdonk, M. L., Cole, J. C., Hartshorn, M. J., Murray, C. W., and Taylor, R. D. (2003) Improved protein-ligand docking using GOLD. *Proteins: Struct., Funct., Genet. 52*, 609−623.

DOI: 10.1021/acschemneuro.5b00271
ACS Chem. Neurosci. 2016, 7, 185−195